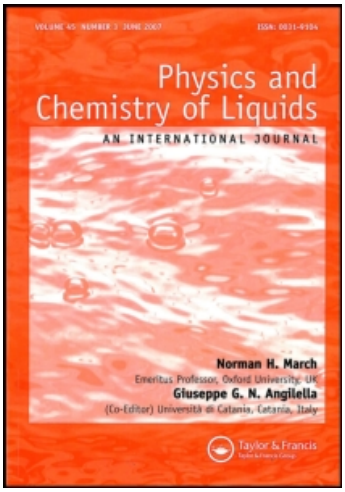

Physics and Chemistry of Liquids
Publication details, including instructions for authors and subscription information:
http://www.informaworld.com/smpp/title~content=t713646857

Collective Modes and Many Body Forces in Fluids: An Experimental Study

P. A. Egelstaff[a]
[a] Department of Physics, University of Guelph, Guelph, Ontario, Canada

To cite this Article Egelstaff, P. A.(1987) 'Collective Modes and Many Body Forces in Fluids: An Experimental Study', Physics and Chemistry of Liquids, 16: 4, 293 — 305
To link to this Article: DOI: 10.1080/00319108708078531
URL: http://dx.doi.org/10.1080/00319108708078531

Phys. Chem. Liq., 1987, Vol. 16, pp. 293-305
Phtocopying permitted by license only

Printed in the United Kingdom

Collective Modes and Many Body Forces in Fluids: An Experimental Study

P. A. EGELSTAFF

Department of Physics, University of Guelph
Guelph, Ontario, Canada

(Received 2 October 1986)

In recent years a number of high quality measurements, at different state parameters, of the dynamic structure factor have been made. These measurements justify two new interpretive approaches. In the first we deduce the magnitude and frequency dependence of the memory function of the current-current correlation function without performing the theoretically correct, but errorful, Fourier–Laplace double transform procedure. This can be achieved[1,2] at a number of special points, and is essentially a direct measurement of this quantity in momentum-frequency space. For the first time the properties of collective modes in fluids can be discussed in a systematic way and this is done for dense krypton gas and for liquid argon.

The same data on krypton and argon may be used to assess the role played by many body forces in dynamic properties because the true pair interaction potentials for these cases are accurately known. Thus in the second approach a high quality computer simulation for krypton, using the true pair potential, is compared to the experimental spectra over an appropriate range of momentum transfer[3,4]. Anomalous effects are observed over the same ranges as novel memory function effects were observed, and are related to the onset of collective mode behaviour.

1 INTRODUCTION

Although short wavelength collective effects in disordered systems are difficult to investigate experimentally, there are a number of theories describing their behaviour. Because one of the most informative experimental quantities is the dynamic structure factor, $S(Q, \omega)$ or Fourier transform of the time dependent pair correlation function, these

theories often present $S(Q, \omega)$ in a form which exhibits collective behaviour explicitly. The most common expression is

$$S(Q, \omega) = \frac{S(Q)}{\pi} \frac{\omega_0^2 \operatorname{Re}\{M(Q, \omega)\}}{|\omega_0^2 - i\omega M(Q, \omega) - \omega^2|^2} \tag{1}$$

where $\hbar Q$ and $\hbar\omega$ represent the momentum and energy used to excite the system. $M(Q, \omega)$ is a (complex) damping function, or a memory function for the current-current correlation function or can be given other meanings. The frequency ω is conveniently expressed in terms of the root mean square frequency $\omega_0 = \sqrt{k_B T Q^2 / M S(Q)}$, where $S(Q)$ is the static structure factor and M the atomic mass.

The damping function can, in principle, be determined from data on $S(Q, \omega)$. Several theories suggest that the real and imaginary parts of $M(Q, \omega)$ are simpler functions of Q and ω, than the dynamic structure factor itself. The interesting physical information about collective behaviour is contained in $M(Q, \omega)$, according to this view. Egelstaff and Gläser[1] point out that an even simpler function is the inverse function

$$\sigma(Q, \omega) = \frac{M(Q, \omega \to 0)}{M(Q, \omega)} \tag{2}$$

and in terms of this function Eq. (1) may be rewritten as (with $\sigma = \sigma_1 + \sigma_2$)

$$\omega_0 S(Q, \omega) = \frac{S(Q)}{\pi} \frac{\sigma_1 / c}{\left| \frac{\sigma}{c}(1 - x^2) + ix \right|^2} \tag{3}$$

where $x = \omega/\omega_0$, $c = \pi\omega_0 S(Q, \omega \to 0)/S(Q) = M(Q, 0)/\omega_0$ and $\sigma/c = \omega_0/M(Q, \omega)$. They also point out that in many experimental situations the frequency range of $M(Q, \omega)$ or $\sigma(Q, \omega)$ is much wider than that of $S(Q, \omega)$ so that the measured data do not contain enough information to allow the integral relationship between the real and imaginary parts of $M(Q, \omega)$ to be exploited. For this reason it is necessary to solve Eq. (3) for the two functions independently. This seemingly impossible task was accomplished by Egelstaff and Gläser[1,2] by taking advantage of the mathematical properties of $\sigma(Q, \omega)$ and of Eq. (3). Their method will be summarized in the next section.

In Section 3 some experimental data on dense krypton gas and on some fluid states of argon will be presented. The behaviour of σ will be discussed in terms of collective effects. Computer simulation results[3,4] for two of the states of krypton will also be presented. Because these results were obtained using the true pair potential for krypton, the

differences between them and the experimental results arise from the many-body potential terms omitted from the simulation. Thus the effect of these terms may be observed in both $S(Q, \omega)$ and $\sigma(Q, \omega)$.

2 THEORETICAL COMMENTS

Equations (1) and (3) are written in a form such that if $M(Q, \omega)$ is small, $S(Q, \omega)$ will exhibit the sharp side peak characteristic of a well defined collective mode. For larger values of $M(Q, \omega)$, or smaller values of $\sigma(Q, \omega)$, the mode is broadened and its definition is not well specified. If the frequency dependences of σ_1 and σ_2/ω are slight, they may be assumed to be approximately independent of frequency in the neighbourhood of the frequency of the mode. In order to define a mode, we shall represent $S(Q, \omega)$ as the sum of three Lorentzians (a central peak and two side peaks) with almost constant coefficients in the neighbourhood of the mode frequency. This expression is

$$\pi S(Q, \omega) = \frac{A_0 z_0}{\omega^2 + Z_0^2} + \frac{2\{(A_{SR}Z_S + A_{Si}\omega_S)(\omega_S^2 + Z_S^2) + (A_{SR}Z_S - A_{Si}\omega_S)\omega^2\}}{\{(\omega + \omega_S)^2 + Z_S^2\}\{(\omega - \omega_S^2) + Z_S^2\}} \tag{4}$$

where A_0 and Z_0 are the amplitude and the width of the central peak and $A_{SR} + iA_{Si}$ are the complex amplitudes of side peaks for modes of frequency $\omega_S + iZ_S$. Any reasonable definition of a mode may be expressed in terms of these parameters. For example Gläser and Egelstaff[2] suggest an acceptable definition would be

$$A_{SR} > 0 \quad \text{and} \quad \omega_S > Z_S \tag{5}$$

Because there are more parameters in Eq. (4) than in Eq. (3), we may write any condition such as (5) as a relationship between σ_1/c and σ_2^0/c (where $\sigma_2^0 = \sigma_2/x$). Thus a measurement of σ_1 and σ_2 at a frequency near ω_S is sufficient to determine whether the condition (5) is satisfied, which is one example of the utility of a measurement of σ.

To solve Eq. (3) for $\sigma = \sigma_1 + i\sigma_2$ in frequency space without using Laplace transform methods, Egelstaff and Gläser[1] wrote it as a quadratic equation in σ_1 and σ_2. Then by noting that σ_1 and σ_2/ω were real, continuous single-valued functions of ω (and $\sigma_1 > 0$ and $\sigma_2 > 0$ at large ω), and by assuming that they were slowly varying functions of ω (so that only the zero and first derivatives with respect to ω need by considered at any point) they solved this equation at six widely spaced

frequencies. These special frequencies cover a range wider than covered by existing $S(Q, \omega)$ measurements, although they do not extend over the complete range of $\sigma(Q, \omega)$. However, usually four or five may be determined from existing experiments, and a reasonable improvement in the quality and extent of the data may allow the higher frequency points to be determined.

Their solutions are (where $n_0 = S(Q)/\pi\omega_0 S(Q, \omega)$)

$$\text{at } x = 0; \quad \sigma_1 = 1$$

$$\sigma_2^0 = \left[2 + \left\{\frac{1}{n_0}\frac{\partial n_0}{\partial x^2} - \frac{1}{\sigma_1}\frac{\partial \sigma_1}{\partial x^2}\right\}_{x=0}\right]^{1/2} - c$$

$$\text{at } x = 1; \quad \sigma_1 = c/n_0$$

$$\frac{\sigma_2^0}{c} = \frac{1}{2}\left[1 - \left(\frac{1}{n_0}\frac{\partial n_0}{\partial x^2}\right)_{x=1}\right] + \left[\frac{1}{\sigma_2^0}\frac{\partial \sigma_2^0}{\partial x^2} - \frac{1}{\sigma_1}\frac{\partial \sigma_1}{\partial x^2}\right]_{x=1}$$

at approximately $x = 0.4$, 1.7 and 3.5

$$\frac{\partial y_2^{\pm}}{\partial x^2} = \frac{\partial \sigma_2^0}{\partial x^2} \quad \text{has a solution } x = x_m,$$

where $y_2^{\pm}(x) = (\pm c)\, n_0 \pm 2x(1 - x^2)/2x(1 - x^2)^2$ is an experimentally determined quantity. This solution determines the value of $y_2^{\pm}(x^m) = \sigma_2^0$, and of $\sigma_1 = n_0 c/2(1 - x_m^2)^2$. This process gives three points.

at approximately $x = 2.5$

$$\frac{\partial y_1}{\partial x^2} = \frac{\partial \sigma_1}{\partial x^2} \quad \text{has a solution } x = x_m,$$

where $y_1 = n_0 c/(1 - x^2)^2$ is another experimentally determined quantity. This solution determines the value of $y_1(x_m) = \sigma_1$ and also $\sigma_2^0 = c/(x_m^2 - 1)$.

Egelstaff and Gläsers[1] solutions imply that the curvature of y_1 or $y_2^{\pm}$ is substantially greater than that of σ_1 or σ_2^0 at $x = x_m$, and that the curvature of σ_2^0 may be neglected over an experimentally significant range of x about $x = 0$ or 1. These conditions are found to hold in practice. As an initial approximation they assumed that $\partial\sigma_1/\partial x^2$ and $\partial\sigma_2^0/\partial x^2$ were negligible, and then used the initial value to estimate these derivatives. Frequently it was found that the initial solution was accurate enough in view of the experimental errors on y_1 and $y_2^{\pm}$. This method allows the real and imaginary parts of the damping function to be measured for the first time, and because algebraic results only are

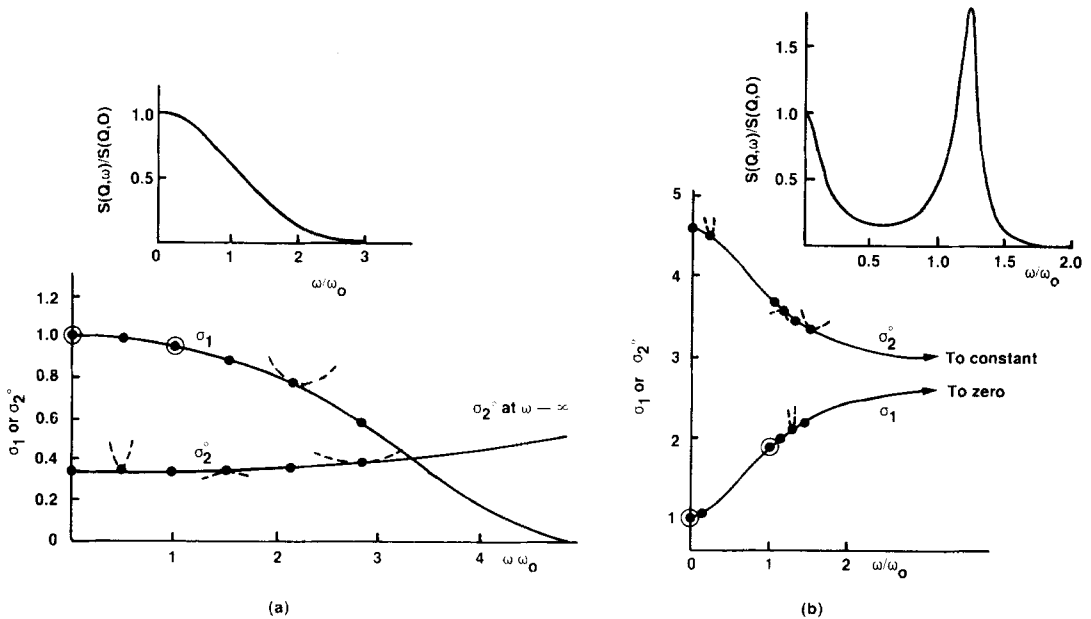

Figure 1 Illustrative examples of how the inverse function $\sigma(Q, \omega)$ is measured. The full lines are σ_1 or σ_2^0 and the dashed lines are y_1 or y_2. (a) For a high Q we have Gaussian shaped $S(Q, \omega)$, σ_1 falls from 1 at $\omega = 0$ to zero at $\omega \to \infty$, while σ_2^0 increases between two constant values. For σ_1 the points marked ⊙ are determined algebraically from $S(Q, \omega)$ while one point is determined by the tangent condition. For σ_2^0 three points are determined by the tangent condition. (b) Similar to (a) for an example of Brillouin scattering at very low Q. In this case σ_1 rises at low ω while σ_2^0 falls: for high ω beyond the limit of the $S(Q, \omega)$ data, σ_1 decreases to zero and σ_2^0 increases to a constant level. Also in this case the six measured points fall into two groups, covering the ω regions where $S(Q, \omega)$ has maximum intensity.

used it also allows the errors in the derived quantities to be related to the errors in $S(Q, \omega)$.

As an example[1], we show in Figure 1 models of $S(Q, \omega)$ for high Q and low Q together with the calculated σ_1 and σ_2^0 functions using the integral method. The six points obtained through the above analysis are marked on these curves, as are (by dashed lines) the functions y_1 and $y_2^{\pm}$. It can be seen that for the Gaussian $S(Q, \omega)$ the six points are distributed in an approximately uniform way along the x-axis, whereas for the Brillouin model they are bunched in regions of high intensity in $S(Q, \omega)$. In both cases they extend to a region of negligible intensity in $S(Q, \omega)$, and provide a reasonable representation of the σ curve over the useful range of ω. However it is evident that for real data extending to about 2% of the maximum intensity, a large part of σ_1 or σ_2^0 would lie beyond the ω-limit in $S(Q, \omega)$. In further support of their approach Egelstaff and Gläser[1] give analytical expressions for σ_1 and σ_2^0 which may be used with any smooth function fitted to the data and extrapolated to large ω. This procedure allows an estimate of the shape of σ_1 and σ_2^0 to be obtained, and so checks the consistancy of the analysis.

Finally, we note that this method of data reduction is not unique to $S(Q, \omega)$ and could be employed in a number of other experimental cases. For example, if a generalized Brownian motion equation is used to describe the motion of an atom (see Ref. 9, Eq. 40), the generalized (complex) diffusion coefficient $D(Q, \omega)$ is given by

$$D(Q, \omega) = \sigma/\pi Q^2 S_s(Q, 0)$$

This illustrates the physical meaning of σ, which may apply to the coherent case over a suitable range of Q.

3 EXPERIMENTAL RESULTS

Gläser and Egelstaff[2] consider a number of $S(Q, \omega)$ experiments which include dense krypton gas (ρ = 10.6 and 13.8 atoms/nm^3) at 297 K, and expanded argon liquid at 120 K (ρ = 17.6 and 20.1 atoms/nm^3). They found that in every case for Q above the principal maximum in $S(Q)$ and for all measured Q's for low density cases, the dependence of σ_1 and σ_2^0 on frequency was very slight so that they were constants within the experimental errors in many cases. We shall compare some of these results with a computer simulation of krypton (Egelstaff *et al.*[3] and Salacuse *et al.*[4], respectively), and with other argon experiments by Verkerk[5] and Sköld *et al.*[6] at 120 K and 85.2 K respectively and at a common density of 21.5 atoms/nm^3. The frequency dependence of these

data is not discussed, but points at different frequencies (see Figure 1) are selected to illustrate particular questions.

a) Krypton: At the gas density 10.6 atoms/nm^3 the real part σ_1 is close to unity for $\omega < 2\omega_0$ and $0.4 < Q < 3.2\text{A}^{-1}$ as illustrated in Ref. 2. The imaginary part, σ_2^0, is ~ 0.3, and varies with Q having a minimum for Q near 1.3A^{-1}. The computer simulation data[3] for this state show a similar behaviour for σ_1 and for the overall level of σ_2^0. But the minimum in σ_2^0 is near 1.8A^{-1} and appears to be narrower, although improved simulation data are needed. Because the simulation was carried out with a realistic pair potential for krypton these differences

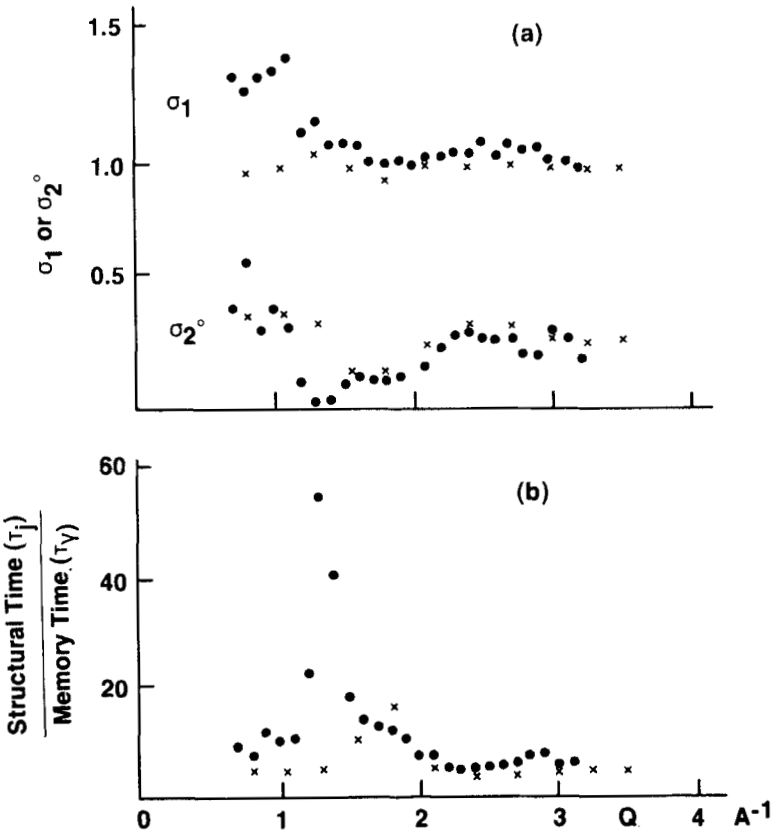

Figure 2 (a) The real and imaginary parts of the inverse function $\sigma(Q, \omega)$ for dense krypton gas at 297 K and $\rho = 13.8$ atoms/nm^3. The circles denote the experimental values while the crosses denote the molecular dynamics simulation[4]. (b) The ratio of *mean times for structural relaxation* (τ_J) *to that for memory relaxation* (τ_γ), which is related[1] to the real and imaginary parts of σ as $\omega \to 0$. This ratio is shown for both the experimental and simulation data.

might be attributed to many body effects. They are larger and more significant, however, at the higher density of 13.8 atoms/nm^3. This is shown in Figure 2a, where σ_1 and σ_2^0 for small ω are plotted against Q. The experimental and simulation results are similar at high Q with values similar to figure 1a. At low Q they show effects reminiscient of the change in intensity between figures 1a and 1b. Also for $Q < 1.3\text{A}^{-1}$, there is a sharp difference between the two sets of data. This is perhaps more evident in Figure 2b where the ratio[1] of mean times for the intermediate scattering function and the memory or damping function are plotted. There is a peak in the experimental data at $Q \sim 1.3\text{A}^{-1}$ which is not evident in the simulation; and is due to the minimum in σ_2^0 at this point.

At Figure 3 we show a comparison[4] of $S(Q, \omega)$ itself for $Q = 1.8\text{A}^{-1}$ and smaller values. It is seen that departures from the simulation occur for $Q = 1.3\text{A}^{-1}$ and that here the experimental curves are sharper. The difference becomes large as Q becomes smaller, and suggests that a side-peak will be seen at slightly lower Q. We show in Figure 4 that, using condition (5), collective modes are strongly damped at $Q = 1.3\text{A}^{-1}$ and are allowed to propagate at lower values of Q. In the cases of the two simulations and the 10.6 atoms/nm^3 experiment, none of the data for $Q \geq 0.6$Å satisfy (5). If both the experimental and simulated data are correct, these results show that many body forces slow down longitudinal atomic motions and encourage the propagation of collective modes.

b) Argon: Results for the densities 17.6 and 20.1 atoms/nm^3 have been published in Ref. 2. The real part σ_1 is close to unity for all experimental values of Q and ω, while the imaginary part is almost independent of ω. Its dependence on Q is shown in Figure 5 (for the second frequency point in Figure 1) and compared to that for argon at the triple point. Although the triple point data[6] are not recent and are of lower quality, it is clear that both σ_2^0 and σ_1 change significantly with the change of state. A smooth line has been drawn through the higher quality data, for the sake of clarity. The data of Verkerk[5] at the triple point density and a temperature of 120 K are shown also. While they do not extend to the higher Q values, they are sufficient to show that a small change of density at 120 K is not significant. The trend at low Q is for increasing values with decrease of temperature, and this suggests the onset of collective modes. This point was made in a quantitative way in Figure 4, where the locus of the data relative to the condition (5) is shown. At low Q (marked on the figure) this condition is satisfied.

Finally for any pair of values of (σ_1 and σ_2^0) the collective mode frequency (ω_s in Eq. (4)) may be calculated. These data are shown in

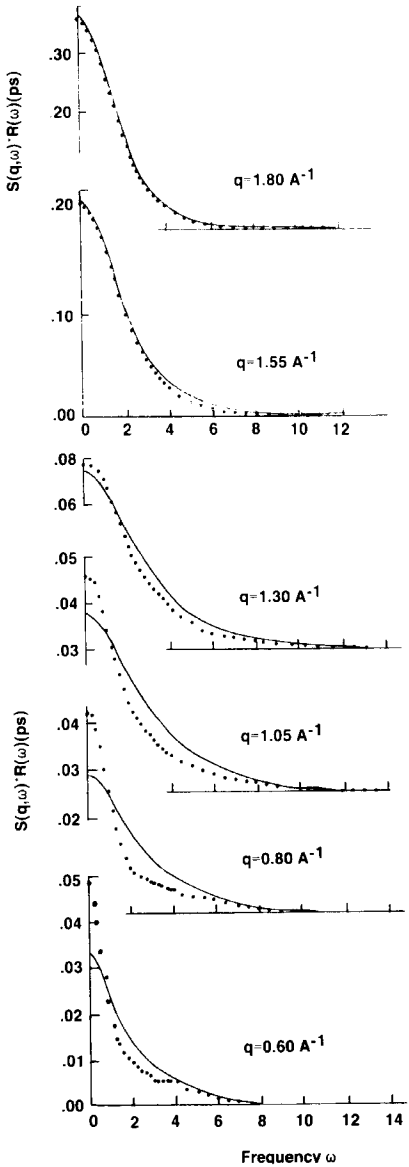

Figure 3 The dynamic structure factor $S(Q, \omega)$ folded with the experimental resolution function $R(\omega)$ for the experimental krypton data[4] (shown by solid circles) and the simulation data[4] (shown by the full line). The Q are taken from the peak of $S(Q)$—at $1.8A^{-1}$ to lower values.

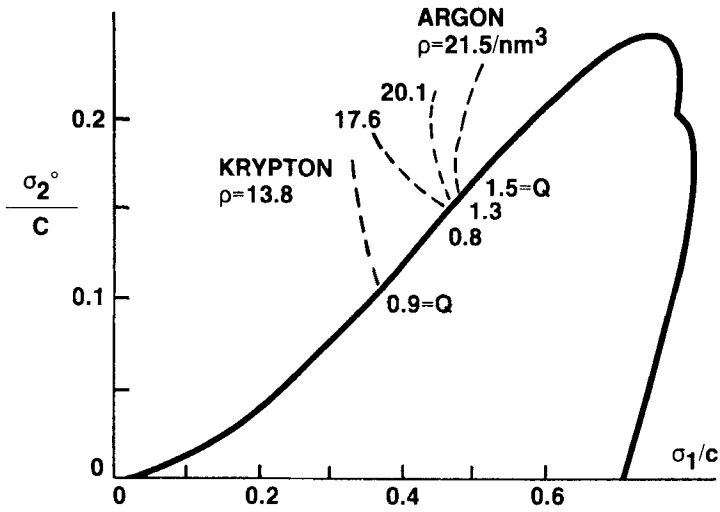

Figure 4 The real and imaginary parts of the inverse function plotted against each other. The condition (5) for propagating modes is shown as a full line-points lying inside the line violate this condition. Dashed lines through the experimental data on krypton and argon are shown (densities and Q values at the intersection with the full line are marked). The data for the two computer simulations of krypton all lie inside the full line, as do the data for krypton at 10.6 atoms/nm^3.

Figure 6 for the densities 20.1 and 17.1 atoms/nm^3 at 120 K and also for the triple point data. The frequency chosen was the fourth point in Figure 1, which is close to ω_S. The condition (5)—Figure 4—would allow modes over a small region of this figure; other conditions might allow a wider range. It is clear that while the general level is similar for all sets of data, there is a difference at $Q \sim 2A^{-1}$ which is the position of the principal maximum of $S(Q)$. In the 17.1 atoms/nm^3 case the modes are overdamped, while at the triple point they are not. The 20.1 atoms/nm^3 case lies between the other two. For Q near the maximum of $S(Q)$ the ratio increases as σ_2^0 decreases, and on Figure 4 they would move towards the overdamped region. Thus in this case the ratio ω_S/ω_0 rises before the overdamped region is reached, which would be consistant with the interpretation of the principal maximum in $S(Q)$ as a point where the momentum given to the system ($\hbar Q$) may be shared between the system as a whole and "transverse or shear modes". This approximation, which is similar to that made for phonons in crystals, leads[7] to significant intensity for scattering at frequencies far away from zero.

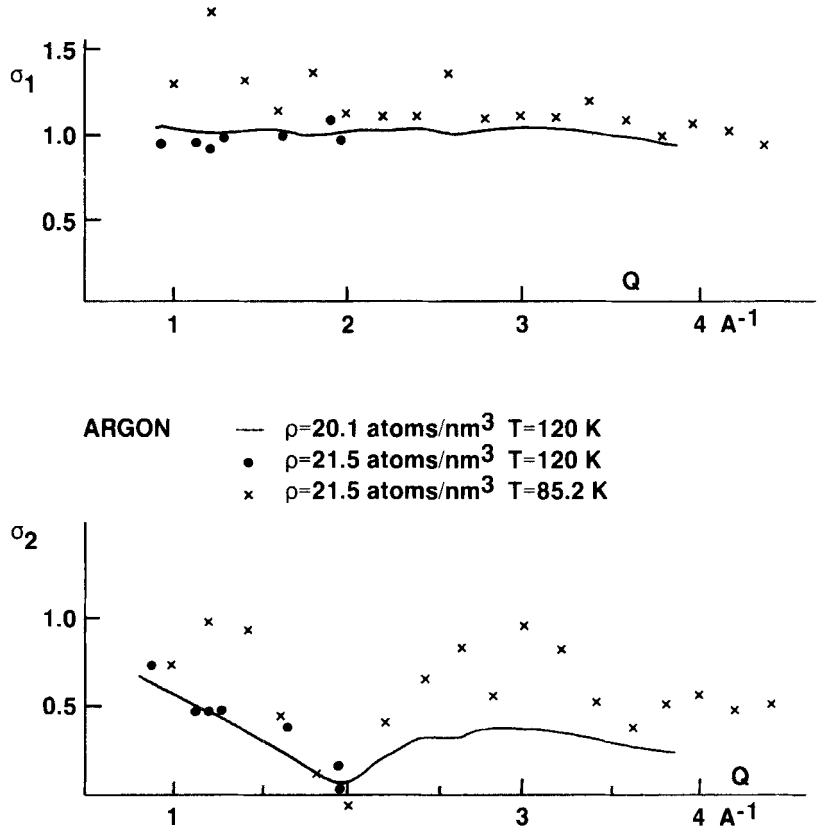

Figure 5 The real and imaginary parts of the inverse function for dense liquid argon (full line[2] is for $\rho = 20.1$ atoms/nm^3 and 120 K, while crosses are for $\rho = 21.5$ atoms/nm^3 and 85.2 K and solid circles for this density at 120 K). These data are for the second frequency point in Figure 1.

4 CONCLUSIONS

A new method of measuring the real and imaginary parts of a response function was proposed[1] and tested on experimental data[2]. In this paper this method is applied in several further cases in an attempt to find the conditions leading to the propagation of collective modes. The conclusions are largely independent of the particular condition used to show the existence of a mode, since all reasonable conditions, proposed in Refs 1 or 2, block out areas in the same part of Figure 4.

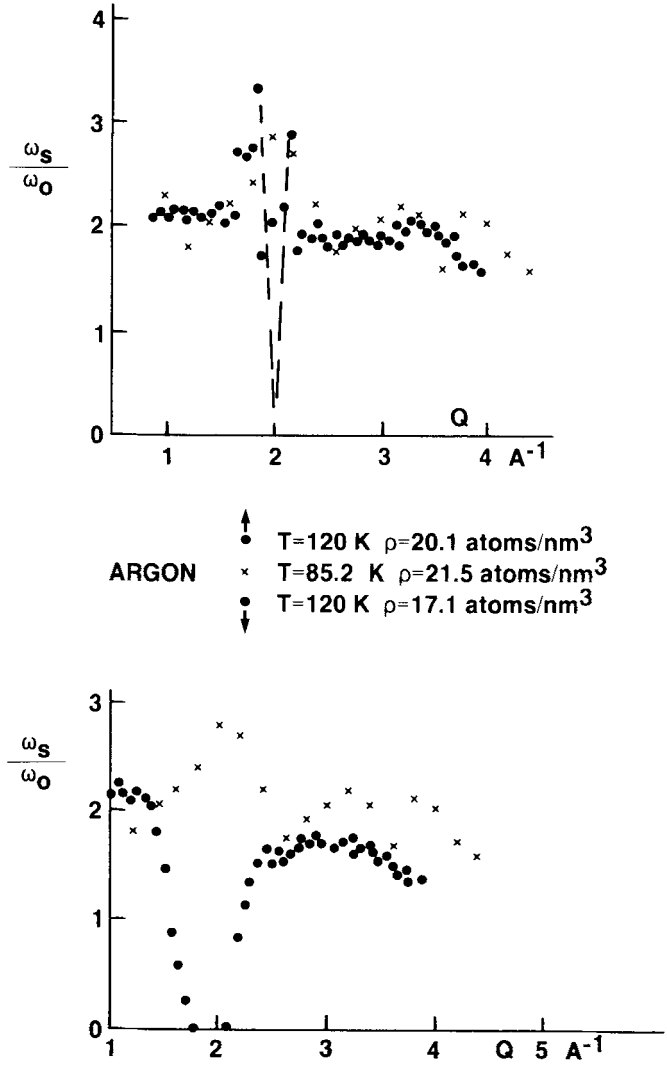

Figure 6 The ratio of collective mode frequency ω_S to the root mean square frequency ω_0 for liquid argon at the two temperatures. Solid circles show data at $\rho = 20.1$ or 17.1 atoms/nm^3 and 120 K, while crosses show data at $\rho = 21.5$ atoms/nm^3 and 85.2 K. These data are for the fourth frequency point shown in Figure 1, which is close to ω_S. The dashed lines indicate the trend of the solid circles near the principal peak of $S(Q)$.

It was demonstrated that for dense krypton gas the on-set of collective mode behaviour occurs for $Q < 0.9$ Å, whereas in the computer simulation no such effect was seen. This was attributed to the contribution from many body terms in the interatomic potentials. In the case of argon trends similar to those in krypton were seen, and the onset of collective modes showed the expected greater likelihood for increases in density and decreases in temperature. However these trends have been made quantitative by the new method. The overdamped behaviour seen in expanded liquid argon ($\rho = 17.1$ atoms/nm^3 in Figure 6) for Q near the maximum in $S(Q)$ is reversed in dense liquid argon, and this might possibly be attributed to "solid-like" transverse mode effects.

The power of the new method has been demonstrated in two ways. First in providing a vehicle to compare and interpret numerous (8) sets of $S(Q, \omega)$ data, and secondly in providing a way of targeting specific problems in a quantitative way. It is hoped that this will lead to a better understanding of a historically complex subject. To improve the present work requires more and better computer simulations, particularly using the realistic pair potential for argon. If the Lennard-Jones potential gives agreement[8] with the data it is likely that many body forces are significant in argon too. On the experimental side a repetition of some of the experiments is desirable, notably the highest density krypton gas and the triple point argon.

Acknowledgement

I would like to thank Dr. W. Gläser for many helpful discussions on this field and Dr. J. Maxwell for a computer program which performs the analysis for σ_1 and σ_2^0. The Natural Sciences and Engineering Research Council of Canada is thanked for their financial support. Part of this paper was presented at the 16th IUPAP International Conference on Thermodynamics and Statistical Mechanics.

References

1. P. A. Egelstaff and W. Gläser, *Phys. Rev. A.* **31**, 3803, (1985).
2. W. Gläser and P. A. Egelstaff, *Phys. Rev. A.* **34**, 2121, (1986).
3. P. A. Egelstaff, J. J. Salacuse, W. Schommers and J. Ram, *Phys. Rev. A.* **30**, 374 (1984).
4. J. J. Salacuse, W. Schommers and P. A. Egelstaff, *Phys. Rev. A.* **34**, 1516, (1986).
5. P. Verkerk, *Theses 1985 Interuniverstair Reactor.* Inst. Delft, Netherlands.
6. K. Sköld, J. M. Rowe, G. Ostrowski, and P. D. Randolph, *Phys. Rev. A.* **6**, 1107 (1972).
7. J. P. Boon and S. Yip, *Molecular Hydrodynamics* (McGraw-Hill Inc. 1980).
8. A. A. Van Well, P. Verkerk, and L. A. de Graaf, *Interuniversitair Reactor. Inst.* Report 132-82-07 (1982).
9. P. A. Egelstaff, *Rep. Prog. Phys.* **29**, 333 (1966).